

### International Journal of

# INTELLIGENT SYSTEMS AND APPLICATIONS IN ENGINEERING

ISSN:2147-6799 www.ijisae.org Original Research Paper

## Comparative Analysis of High Accuracy Hybrid Models for Mammography Image Classification with and without Segmentation

Sailaja Pendyala \*1, N. Vanamadevi #2, K. Ramanjaneyulu \*#3

**Submitted**:12/03/2024 **Revised**: 27/04/2024 **Accepted**: 04/05/2024

Abstract: Mammography is an essential diagnostic tool for early detection of breast cancer. Advances in deep learning, including transfer learning models and hybrid Convolutional Neural Network (CNN) classifiers, have shown promise in improving diagnostic accuracy. This study compares the classification performance of transfer learning models and a hybrid CNN classifier without segmentation to a dedicated computer-aided diagnosis (CAD) system with segmentation on mammographic images. The objective is to evaluate the effectiveness of standalone models versus integrated CAD systems in detecting breast cancer. The contribution of this paper can be summarised as follows: the initial phase involved preprocessing, which included image contrast improvement technique CLAHE (Contrast Limited Adaptive Histogram Equalization), resizing, normalisation, and image augmentation. The second step is classifying pre-processed images without segmentation using VGG16, MobileNet, ResNet152V2, ResNet50V2, and four hybrid models H1, H2, H3, and H4 as benign and malignant. The suggested hybrid methods exhibit improved performance in comparison to the corresponding transfer learning models, capitalising on the combined benefits of both networks. Furthermore, the incorporation of a probability-based weight factor (w) and threshold value ( $\beta$ ) is essential for achieving optimal hybridisation. The empirically discovered optimal threshold value ( $\beta$ ) improves the speed and accuracy of the system. Significantly, in contrast to conventional deep learning techniques, the suggested framework demonstrates exceptional performance. Finally, the images are segmented using the MultiResUNet++ model, and the obtained segmented masses are classified using the four hybrid models. In this paper, the classification of the mammography images was compared with and without segmentation. The experimental results demonstrate the superiority of the proposed VGG16- ResNet50V2 scheme over the current state-of-the-art methods, with a precision of 98.94%, accuracy of 98.42%, Recall of 97.89%, F1 Score of 98.41% and ROC score of 98.54%.

Keywords: CAD, Hybrid model, Mini DDSM, MultiResUNet, UNet++

#### 1. Introduction

With the current state of affairs, breast cancer has emerged as one of the most prevalent forms of malignant tumours in females, and the incidence of this disease is increasing in both developed and developing nations. In clinical practice, malignant tumors are typically classified as positive, while benign tumors are classified as negative. Several imaging technologies, including mammography as examinations, Computed Tomography (CT), photoacoustic scans, nuclear magnetic resonance imaging, and microwave scanning [5], are used, and others, are currently being utilised to diagnose breast cancer [1,2]. Out of all these methods, mammography is one of the most effective methods for identifying breast cancer [3]. mammograms, the most prominent signs of breast cancer are masses and calcifications. Both of these are considered to be symptoms of the disease. When viewed from the mass, benign tumours often have a spherical, smooth, and

<sup>1</sup>Research Scholar, Department of Electronics and Instrumentation Engineering, Faculty of Engineering and Technology, Annamalai University, Annamalai Nagar, Tamil Nadu, India. generally transparent appearance. Calcification can be defined by several qualities such as a rougher shape, a grainy shape, a popcorn-like shape, or a ring-like shape. Furthermore, the calcification exhibits a greater density and a more extensive dispersion. Malignant tumours typically exhibit a needle-like morphology with irregular and frequently indistinct margins. Malignant tumours are very dangerous. There are a variety of forms and sizes, and the distribution of calcification is frequently dense or packed in a linear pattern [4]. The calcification morphology is primarily composed of microscopic sand-like particles that are either linear or branching. Medical experts face difficulties in accurately diagnosing early breast cancer based on mammography scans due to the complexity and low contrast of the images. Given this, it is imperative to enhance the diagnostic capabilities of medical practitioners by employing the computer-aided diagnostics (CAD) system that relies on deep learning.

The advancement of processing digital images and Artificial Intelligence (AI) technologies has resulted in a notable transformation in the medical domain, specifically breast cancer detection [5] and diagnosis. Computer-aided detection and diagnosis (CAD) systems are now considered valuable tools that assist radiologists in accurately categorising benign and malignant breast tumours [6]. This improvement is not merely theoretical but a practical and urgent scientific problem that healthcare specialists are

<sup>&</sup>lt;sup>2</sup>Department of Electronics and Instrumentation Engineering, Faculty of Engineering and Technology, Annamalai University, Annamalai University, Annamalai Nagar, Tamil Nadu, India.

<sup>&</sup>lt;sup>3</sup>Department of Electronics and Communication Engineering, P.V.P. Siddartha Institute of Technology, Kanur, Vijayawada-520007

<sup>\*</sup> Corresponding Author Email: sailupendyala@gmail.com

 $<sup>\#\</sup> Corresponding\ Author\ Email: \underline{vanamadevinraju@gmail.com}$ 

<sup>\*#</sup> Corresponding Author Email: kongara.raman@gmail.com

actively tackling. CAD [7] systems function by examining mammography pictures to detect patterns and irregularities that could suggest the existence of tumours. Algorithms and machine learning approaches are employed to aid radiologists in making accurate and prompt diagnoses. This technique has gained prominence and importance due to its capacity to enhance the precision and effectiveness of breast cancer detection. In addition, CAD systems are used to identify and categorize microcalcifications and masses in mammography pictures. Microcalcifications are minuscule accumulations of calcium that can serve as early signs of breast cancer. Computer-aided detection (CAD) systems [7] can assist radiologists in identifying these minor alterations that may go unnoticed during a human examination. Incorporating digital image processing and artificial intelligence technology into CAD systems

fundamentally transformed breast cancer diagnostics, enhancing its precision, efficiency, and reliability. Segmenting masses [8] from mammograms is difficult because of their various properties, including shape, border, texture, and density. Segmenting mass using machine learning requires carefully selecting features, which can be time-intensive. On the other hand, deep learning approaches enable the automatic acquisition of features straight from the training data. Utilizing fully convolutional neural networks, such as U-Net [9], has proven highly successful in biomedical picture semantic segmentation. U-Net is a supervised learning approach that incorporates encoder and decoder layers. Over time, several versions of U-Nets have appeared, incorporating transfer learning techniques, skipconnection configurations, attention processes, and visual transformer-based U-Net structures [10],[11],[12],[13],[14].

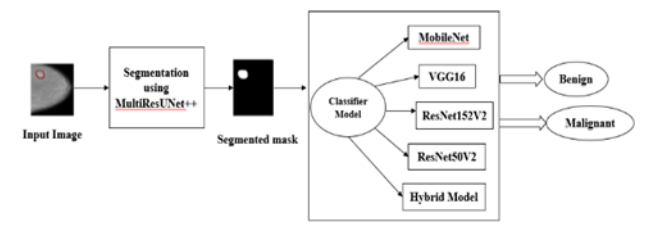


Fig.1. Proposed frame work

This research makes two important contributions: a classification phase that employs multiple deep models, and a segmentation phase that comes before the classification shown in Fig 1. Initially, various models such as VGG16, MobileNet, and ResNet152V2, ResNet50V2 and hybdird models are utilized to categorize the images in our Mini-DDSM dataset as either benign or malignant. Furthermore, the MultiResUNet++ modified U-Net model is employed in the segmentation phase to extract the Region of Interest (ROI). This step is crucial in optimizing the images for input into the classification phase and the system's performance. Following the segmentation step, our deep-learning models identify the segmented images as benign or malignant. Data augmentation is used on dataset to address the limited availability of datasets. In addition, transfer learning is employed to reduce both the time required and the computational resources consumed.

#### 2. Related Work

Machine learning surpasses the traditional method of manually creating techniques. It aids in the identification of the most crucial elements. Deep learning is crucial for improving advancements in biomedical engineering, namely in the area of Deep Convolutional Neural Networks (CNNs), which have demonstrated exceptional efficiency when implemented. Shrestha et al. devised a new algorithm to characterize deep learning [16]. J. Arevalo et al. [17] explain several Convolutional Neural Networks (CNNs) used for mass detection. The researchers conducted their experiments utilizing the Breast Cancer Digital Repository

Film Mammography (BCDR-FM) dataset. In their research, D. Abdelhafiz et al. [18] introduced a system that utilized a pre-trained Convolutional Neural Network (CNN) on the DDSM database. The authors, L. Tsochatzidis et al. [19], have developed a breast cancer classification algorithm from the beginning. This algorithm enhances the capability to differentiate between normal and abnormal breast tissue by utilizing deep-learning medical imaging technology.

The U-Net model is the primary model used for image segmentation. O. Ronneberger et al. proposed a U-Net model to segment biomedical images [9]. N. Alam et al. [20] devised an automated method for segmenting biological pictures. The researchers manually extracted the region of interest (ROI) and then used a wavelet-based procedure to enhance the spatial picture's frequency. The shape of the calcified area was determined

using a segmentation technique used in the study by S. Duraisamy et al. [21]. The improved U-Net model was used to perform segmentation and extract the region of interest (ROI), with a specific focus on the breast area and the removal of any undesired regions. This approach has been documented in several articles focusing on the classification of breast cancer [22–26].

The data augmentation technique generates additional samples for the training data set by applying random transformations to the existing datasets [27]. This has numerous consequences, such as expediting the convergence process and preventing overfitting. A practical method for tiny datasets is applying simple transformations

such as translation, zooming, flipping, mirroring, rotation, etc. Transfer learning refers to employing a pre-trained model instead of starting the model training process from scratch. Developing the neural network initially requires significant data and computer resources [28]. The classification procedure utilized the following models: VGG16, ResNet152V2, MobileNetV2, ResNet50v2 [29–31, 49].

## 3. Proposed Architecture for Segmentation and Classification

Training data is necessary for the implementation of deep learning models. An automated mass segmentation model necessitates the inclusion of ground truth images that radiologists have annotated. The mini-DDSM dataset is publicly accessible and contains annotations for mammography images [32]. The collection contains cranio-caudal (CC) and mediolateral oblique (MLO) images of both the right and left breast, saved in 16-bit .JPEG format. The dataset includes data on the ground truth provided by specialists for each image, classifying them as either benign or Malignant. The current study randomly selects a subset of 2200 mammography pictures from the Mini-DDSM dataset. This subset is employed to evaluate the efficacy of the suggested model using a limited dataset.

#### 3.1. MultiResUNet++

The MultiResUNet++ architecture is a combination of the

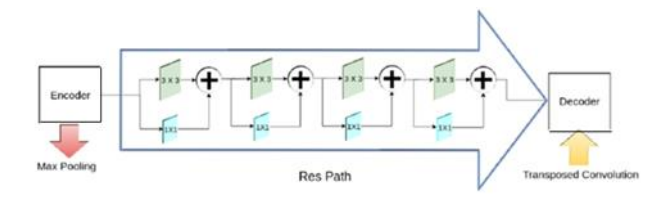


**Fig. 4.** Shows the rp (Respath) that is present in the structure of the MultiResUNet++ model.

MultiResUNet and UNet++ designs. The approach aimed to overcome constraints in both systems, specifically in efficiently managing distant relationships and accurately capturing intricate features in segmentation tasks.

The MultiResUNet++ architecture is a combination of the MultiResUNet and UNet++ designs. The approach aimed to overcome constraints in both systems, specifically in efficiently managing distant relationships and accurately capturing intricate features in segmentation tasks. The architecture of the MultiResUNet++ model is illustrated in Fig 2. MultiResUNet++ preserves the basic encoder-decoder architecture of MultiResUNet while incorporating more connections, influenced by UNet++, to enhance the information exchange between various model layers.

The MultiResUNet++ model incorporates the fundamental UNet structure, which consists of an encoder and a decoder.

The encoder performs downsampling of the input image to extract higher-level features, while the decoder utilises upsampling layers to reconstruct fine-grained information and provide a segmentation mask. Typically, each level of an encoder is composed of convolutional layers, followed by pooling layers. This arrangement helps to improve the extraction of features. MultiResUNet++ is a modified version of UNet++ that includes additional skip connections between the encoder and decoder layers. These connections allow for the seamless combination of low and high-level information, which is beneficial for segmentation tasks.

Additionally, it has a hierarchical structure in which each level of the encoder is connected to the decoder through layered skip connections. This enables the thorough incorporation of characteristics at various scales and facilitates accurately representing local and global contexts. The network's interconnection allows it to overcome difficulties associated with long-range interdependence and the acquisition of fine-grained details in segmentation tasks.

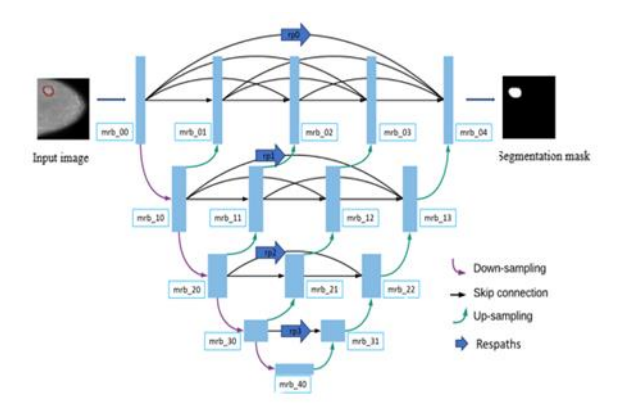


Fig. 2. Structure of MultiResUNet++ model

#### MultiRes Block

The MultiResUNet++ design relies on the MultiRes blocks, depicted in Fig 2. and referred to as multiRes block (mrb), as the fundamental components for its multi-resolution analysis capabilities. The blocks shown in Fig 3. deviate from conventional convolutional layers by incorporating concurrent convolutional processes with different kernel sizes. Furthermore, the progressive increase in the quantity of filters in each subsequent layer allows the network to extract spatial characteristics from various scales with greater efficiency. This novel method not only improves the precision of segmenting but also reduces the limitations of memory, hence optimizing the overall performance.

#### Respath

Moreover, the architecture specifically tackles the semantic disparity that exists between the characteristics of the encoder and decoder in the UNet framework. Fig 2. incorporates Respathways, which are denoted as rp. The ResPath, as shown in Fig 4, incorporates convolutional

layers selectively along shortcut connections to enhance the alignment of features between the encoder and decoder stages. The Respathways, together with residual connections, are crucial for maintaining spatial information during the segmentation process, hence improving the overall resilience and effectiveness of the network.

The U-Net and MultiResUNet architectures establish a direct connection between the encoder and decoder, allowing the decoder to receive feature maps directly from the encoder. MultiResUNet++ incorporates a dense convolution block, with the number of blocks varying depending on the pyramid level. The purpose of this block

is to synchronize the semantic level of encoder feature maps with those in the decoder. The hypothesis is that having a tighter semantic likeness between these feature maps makes optimization easier for the optimizer. MultiResUNet++ differs from UNet and UNet++ in four crucial aspects: 1) The model effectively incorporates MultiRes blocks to extract spatial features from multiple scales. 2) It introduces Respaths to preserve spatial information throughout the segmentation process. 3) MultiRes blocks are used on skip pathways to connect the encoder and decoder feature maps and bridge the semantic gap. 4) Dense skip connections are employed on skip pathways to improve the flow of gradients.

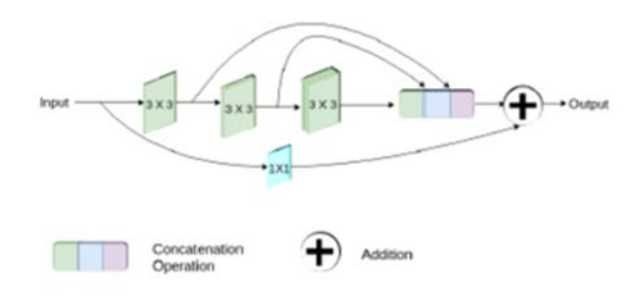


Fig. 3. Shows the mrb that is present in the structure of the MultiResUNet++ model.

#### 3.2. Hybrid Model

In this study, we have employed four novel deep hybrid networks [47], namely H1, H2, H3, and H4, to enhance the precision of breast cancer diagnosis. Fig 5. displays the diagram of the proposed work. This study aims to enhance performance accuracy while improving computing efficiency. P1 and P2 denote the chances of class membership forecasted by the hybrid network's initial classifier. P1 and P2 represent the probabilities of normal and malignant, correspondingly. Class 1 represents benign, while class 2 represents malignant. The weight factor is crucial for ensuring optimal performance and improving computational efficiency. The weight factor (w) is mathematically represented as follows:

$$w = \sum_{k=1}^{u} P_k \log_2(uP_k) \tag{1}$$

for u number of classes.

Given that cancer detection is a problem with two possible outcomes, u is defined as two. The proposed mixed framework amalgamates the benefits of both classifier 1 and classifier 2 networks. The threshold value is essential for attaining an ideal balance between capability and computational effectiveness. When P1=0.5, the probability of the item being assigned to class 1 is 0.5, while the probability of it being assigned to class 2 is likewise 0.5. Here, P1 and P2 represent the probability of class 1 and class 2, respectively. Consequently, it leads to misdiagnosis. When P1 = 0.9, the probability of an item being classed as class 1 is 0.9, while the probability of it being classified as class 2 is 0.1. Similarly, if P1 = 0.1, the probability of an item belonging to class 1 is 0.1,

whereas the probability of an object belonging to class 2 is 0.9. In both scenarios, the likelihood of misclassification (classifier 1) is comparatively lower, resulting in improved classification. In this context, we calculate the value of w based on P1 and P2, as described in Equation (1). The relationship between P1, P2 and w is seen in Table 1. The weight factor (w) remains constant when the values of P1 and P2 are interchanged. Therefore, at w = 0, the chance of misclassification reaches its highest point, with P1 = P2 = 0.5. With an increased value of w, the likelihood of misdiagnosis in classifier 1 is comparatively lower. Therefore, the second network only engages when the first classifier performs relatively subpar. Based on the observation of Fig. 6, it is evident that the second network is only involved when the weight factor (w) is less than or equal to the threshold value  $(\beta)$ . If the weight factor w is greater than  $\beta$ , subsequently, the activation of the second network is unnecessary. The network2 operates exclusively when the network1 exhibits comparatively performance. This maximizes the utilization of the second network by eliminating the requirement to activate both networks for every test image. Applying this notion enhances the suggested framework's computational efficiency and overall performance. Therefore, the threshold value  $(\beta)$  is essential in attaining an ideal balance between performance and computational effectiveness. To fulfill this objective, the value of  $\beta$  is determined by experimental means. To create effective hybrid schemes, two classifiers, namely classifier 1 and classifier 2, are selected from a pool of five base classifiers: VGG16, VGG19, ResNet50V2, MobileNetV2, and ResNet152V2. The hybrid schemes that have been suggested are displayed in Table 2.

**Table 1.** Variation of P1 and P2 with w

P1	P2	W
0.5	0.5	0
0.4070	0.5930	0.025
0.3690	0.6310	0.05
0.3400	0.66	0.075
0.3160	0.6840	0.1
0.2145	0.7855	0.25
0.18	0.82	0.3
0.11	0.89	0.5
0.00001	0.9999	1

**Table 2.** Hybrid Frameworks

Hybrid	Classifier 1	Classifier 2
H1	ResNet152V2	VGG16
H2	ResNet50V2	VGG19
НЗ	MobileNet	ResNet50V2
H4	VGG16	ResNet50V2

#### 4. Results and Evaluation

#### 4.1. Dataset and Preprocessing

The DDSM [41] collection is free. It is distributed by the University of South Florida Computer Science and Engineering Department, Sandia National Laboratories, and MGH [42]. The Mini-DDSM dataset is a sample of the larger DDSM dataset. It may have been chosen to be easy to reach and simple. A popular mammography source is the DDSM. It contains metadata and annotations for several mammography pictures. Researchers can test a small portion of this useful dataset with the Mini-DDSM subset. This study selected 2200 Mini-DDSM tumor-bearing mammograms. After reviewing them, 1810 were randomly selected for training, 200 for validation, and 190 for testing. Images were rotated and turned to increase the training collection. Data utilized to train the models become more stable and diverse.

A poor signal-to-noise ratio in mammograms is unfixable. For accurate identification, preprocessing is crucial. Increasing contrast with Contrast Limited Adaptive Histogram Equalization (CLAHE) helped picture lines stand out. When working with limited datasets like mammograms, adding data made deep learning models

more valuable and dependable. Rotating and flipping were used for augmentation. The model learns stable traits and trends by changing certain sections of the source photographs. It performs better and reduces overfitting. Growing: Many forms can be transformed into pictures. With the revised shape, each is 256 tall and wide. Pictures altered shape (256, 256, 1). A 1 form shows one channel, or a grayscale picture. Before using deep learning to distinguish images, normalization is necessary. The segmentation model must perform properly and stay stable to ensure that the data fed in has the same values. Projects that segment photographs with varied lighting, contrast, and intensity can provide extremely different pixel values. This may hinder learning and reduce segmentation model effectiveness.

#### 4.2. Performance Metrics

The performance of the recommended model was assessed using various metrics, including overall accuracy, specificity, sensitivity, precision, f1-score, confusion matrix. The f1-score value provides a straightforward way to calculate the harmonic mean of recall and precision values. The consideration of extreme instances is the rationale behind the preference for a harmonic mean over a simple mean. In a scenario where a simple average

computation is used, a model that has a recall value of 1 and a precision value of 0 could potentially have a f1-score of 0.5, which can be misleading [43–46]. The mathematical representations are defined in equations (2) to (6) as follows:

$$Accuracy = \frac{TP + TN}{TP + FN + TN + FP} \tag{2}$$

$$Specificity = \frac{TN}{TN + FP} \tag{3}$$

$$Sensitivity(Recall) = \frac{TP}{TP + FN}$$
 (4)

$$Precision = \frac{TP}{TP + FP} \tag{5}$$

$$F1 - Score = \frac{2*Precision*Sensitivity}{Precision + Sensitivity}$$
 (6)

#### 4.3. Experimental Results and Discussion

The discussion includes the segmentation and classification findings, such as the segmentation model's qualitative results, the accuracy plots for training and validation, the plots for IoU and loss, and the plots for ROC and precision and recall curves.

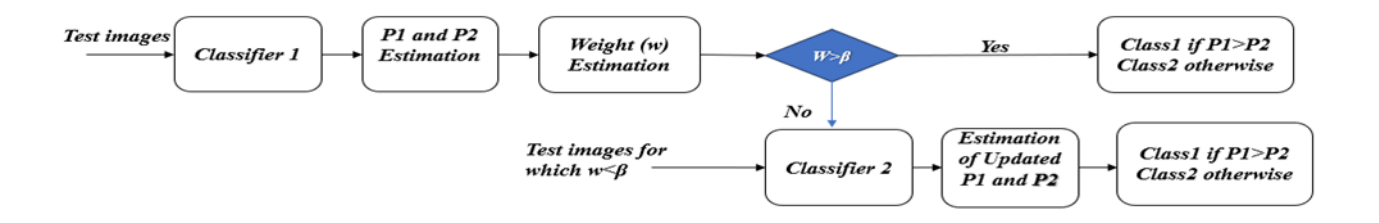


Fig. 5. displays a diagram illustrating the hybrid model that has been proposed.

#### 4.3.1. Segmentation Results

Segmentation using MultiResUNet++ model experimental results attained an accuracy of 99.78%, an

Intersection over Union (IoU) of 97.68%, and a loss value of 0.00113. The plots of training and validation accuracy, training and validation IoU, and loss plots are given in Fig 6., and also the qualitative results are shown in Fig 7.

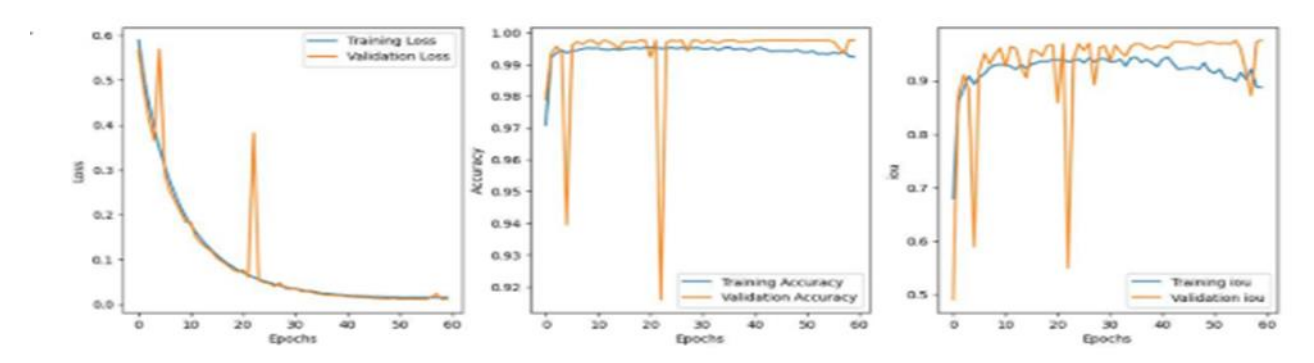


Fig. 6. displays the Loss, Accuracy, and IoU graphs for both the training and validation dataset

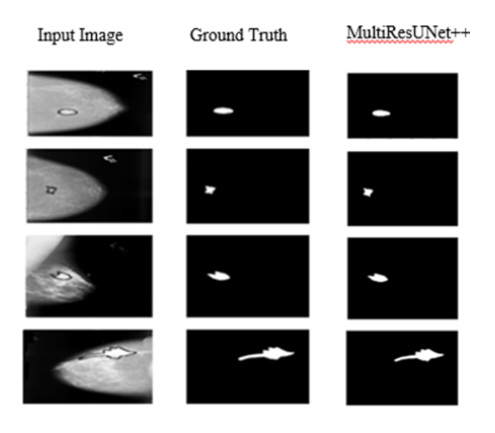


Fig. 7. Qualitative results of MultiResUNet++ showing segmentation of mammogram images

#### 4.3.2. Classification Results

After the segmentation, the resulting images were sent as input to the different classifier models. The performance metrics of these transfer learning models without and with segmentation were compared, as shown in Table 3 and Table 4 respectively, which means the classification output was evaluated both without segmentation and with segmentation. The results showed that the accuracy and ROC measurements improved when the classification was performed after segmentation. The proposed approach is subjected to a quantitative performance study, along with other comparative methods. This analysis is conducted metrics such as, precision, recall, F1 score, specificity, accuracy, and ROC. The comparison table clearly illustrates the superiority of the proposed method, which exhibits greater accuracy and precision than its competitors. The graphical depiction of the results in the mini-DDSM database and the confusion matrix for the H4 model are depicted in Fig 8. and 9, respectively. Based on the provided table, it can be concluded that the suggested hybrid technique performs better than previous techniques in terms of all performance metrics. Specifically, it achieves a precision of 98.94%, accuracy of 98.42%, recall of 97.89%, specificity of 98.95%, F1 score of 98.41%, and

ROC of 99.54%. The threshold value is crucial in both hybridization and achieving optimal outcomes. This value is selected through empirical experimentation. Furthermore, it is necessary to optimize the threshold value to achieve exceptional detection accuracy. Table 5 illustrates the performance comparison when using various threshold values to detect begin or malignant. Based on the data presented in this table, it can be concluded that the proposed hybrid framework performs better with a threshold value of 0.3. Once the threshold value reaches a certain point, performance begins to deteriorate and then remains constant. The proposed hybrid models exploit the second classifier in cases where the performance of the first classifier is below standard, leading to improved success by using the strengths of both basic classifiers: classifiers 1 and 2. However, there is a possibility of false detection occurring when the second classifier, used for testing, also produces erroneous detection. Although the likelihood of this problem occurring is low, it can happen occasionally (in rare cases). Therefore, there is need for additional improvement. The section closes by asserting that the suggested hybrid strategy achieves outstanding performance in categorizing benign-malignant breast pictures on mammograms, while maintaining similar computational costs.

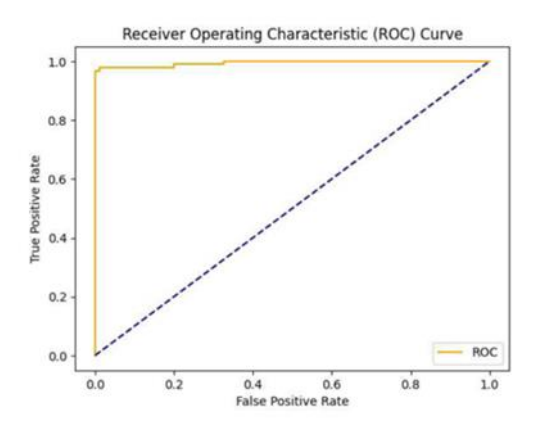


Fig. 9. Displays the ROC curve of H4 model

**Table 3.** Comparison of different transfer learning models classification performance of mammogram images as benign and malignant without segmentation

Classification before Segmentation	Precision	Recall	Accuracy	Specificity	ROC	F1 Score
MobileNet	97.12	91.00	93.38	96.45	98.21	93.56
VGG16	98.23	92.12	94.34	95.85	98.36	95.08
ResNet152V2	98.66	93.81	94. 86	97.78	99.67	95.65
ResNet50V2	98.67	95.56	95.37	98.96	99.81	96.01
H1 model	97.48	96.67	96.45	98.67	98.46	97.76
H2 model	98.33	97.53	97.39	97.89	97.56	97.38

H3 model	98.65	94.89	97.88	98.79	98.79	97.41
H4 model	98.13	97.82	98.19	98.56	99.16	98.32

**Table 4.** Comparison of different transfer learning models classification performance of mammogram images as benign and malignant after segmentation

Classification after Segmentation	Precision (%)	Recall (%)	Accuracy (%)	Specificity (%)	ROC (%)	F1 Score (%)
H1 model	95.88	97.89	96.84	95.79	99.10	96.88
H2 model	97.87	96.84	97.37	97.89	98.89	97.35
H3 model	98.91	95.79	97.37	97.89	99.42	97.33
H4 model	98.94	97.89	98.42	98.95	99.54	98.41

#### 5. Conclusion

This paper presents a novel hybrid deep learning framework that utilizes various deep learning models. The proposed framework employs the MultiResUNet++ architecture for segmentation, while a hybrid model is formed by combining transfer learning models for classification. The hybrid model H4, which combines VGG16 for classifier1 and ResNet50V2 for classifier2, achieves superior

performance. A comparison analysis is conducted to

compare the performance of classification models with and without segmentation. The experimental results show that classification using H4 model without segmentation achieved an accuracy of 98.19%, an ROC of 99.16%, a recall of 97.82%, a precision of 98.13%, and an F1 score of 98.32%. On the other hand, classification with segmentation achieved an accuracy of 98.42%, an ROC of 99.54%, a recall of 97.89%, a precision of 98.94%, and an F1 score of 98.41%. Segmentation enhances the performance of classification, especially when dealing with a tiny dataset.

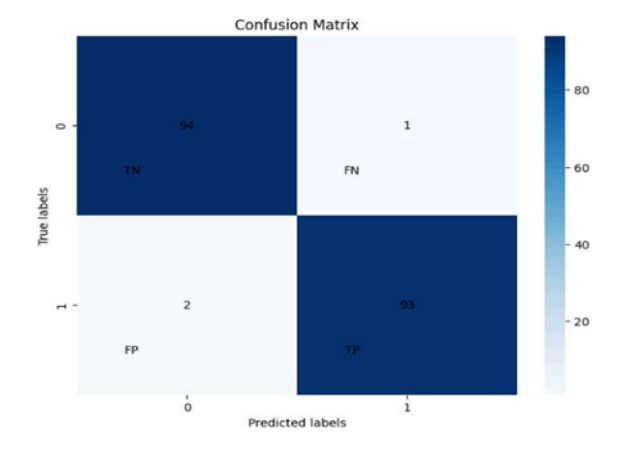


Fig. 8. Confusion matrix for H4 model

Table 5. Performance comparison using various threshold levels for malignancy detection after segmentation

		Precision	Recall	Accuracy	Specificity	ROC	F1 Score
	Model	(%)	(%)	(%)	(%)	(%)	(%)
0.025		95.74	94.74	95.26	95.79	99.18	95.24
0.05		95.79	95.79	95.79	95.79	99.87	95.79
0.075	H1 model	95.79	95.79	95.79	95.79	98.86	95.79
0.1		95.79	95.79	95.79	95.79	98.86	95.79
0.25		95.79	95.79	95.79	95.79	98.86	95.79

0.3		95.88	95.88	96.84	95.79	99.1	96.88
0.5		95.88	95.88	96.84	95.79	99.2	96.88
0.025		97.83	94.74	96.32	97.89	98.56	96.26
0.05		97.85	95.79	96.84	97.89	99.65	96.81
0.075		96.81	95.79	96.32	96.84	98.56	96.3
0.1	H2 model	96.81	95.79	96.32	96.84	98.56	96.3
0.25		97.83	94.74	96.32	97.89	97.45	96.26
0.3		97.87	96.84	97.37	97.89	99.89	97.35
0.5		97.87	96.84	97.37	97.89	99.86	97.35
0.025		98.91	95.79	97.37	98.95	99.21	97.33
0.05		98.91	95.79	97.37	98.95	99.21	97.33
0.075	***	98.91	95.79	97.37	98.95	98.87	97.33
0.1	H3 model	98.91	95.79	97.37	98.95	99.11	97.33
0.25		96.81	95.79	96.32	96.84	98.64	96.3
0.3		97.85	95.79	96.84	97.89	99.49	96.81
0.5		97.85	95.79	96.84	97.89	99.49	96.81
0.025		97.89	97.89	97.89	97.89	99.12	97.89
0.05		97.89	97.89	97.89	97.89	99.24	97.89
0.075		97.89	97.89	97.89	97.89	99.24	97.89
0.1	H4 model	98.94	97.89	98.42	98.95	98.89	98.41
0.25		98.94	97.89	98.42	98.95	99.46	98.41
0.3		98.94	97.89	98.42	98.95	99.54	98.41
0.5		98.92	96.94	97.89	98.95	99.54	97.87

#### References

- [1] X. Xiao, L. Xu, B.Y. Liu, Three-dimensional simulation for early breast cancer detection by ultrawideband, Acta Phys. Sin. 62 (4) (2013) 221–229;(b) J. Ferlay, H.R. Shin, F. Bray, et al., Estimates of worldwide burden of cancerin 2008: globocan 2008, Int. J. Cancer 127 (12) (2010) 2893–2917.
- [2] L. Guang-Dong, Three-dimensional microwaveinduced thermos acoustic imaging for breast cancer detection, Acta Phys. Sin. 60 (7) (2011)074303– 074913.
- [3] J.M. Timmers, H.J. van Doorne-Nagtegaal, H.M. Zonderland, et al., The BreastImaging Reporting and Data System (BI-RADS) in the Dutch breast cancer screening program: its role as an assessment and stratification tool, Int. J.Med. Radiol. 22 (8) (2012) 1717–1723.
- [4] N.V.S.S.R. Lakshmi, C. Manoharan, An automated system for classification of micro calcification in

- mammography based on Jacobi moments, Int. J. Comput.Theory Eng. 3 (3) (2011) 431–434.
- [5] Gautam, A. Recent advancements of deep learning in detecting breast cancer: a survey. Multimedia Systems 29, 917–943 (2023).
- [6] Wang L (2024) Mammography with deep learning for breast cancer detection, Front. Oncol. 14:1281922
- [7] Yoo, S., Lee, S., Kim, S. *et al.* Integrating deep learning into CAD/CAE system: generative design and evaluation of 3D conceptual wheel. *Struct Multidisc Optim* **64**, 2725–2747 (2021).
- [8] Vivek Kumar Singh, Hatem A. Rashwan, Santiago Romani, Farhan Akram, Nidhi Pandey, Md. Mostafa Kamal Sarker, Adel Saleh, Meritxell Arenas, Miguel Arquez, Domenec Puig, Jordina Torrents-Barrena, Breast tumor segmentation and shape classification in mammograms using generative adversarial and convolutional neural network, Expert Systems with

- Applications, Volume 139, 2020,112855, ISSN 0957-4174.
- [9] O. Ronneberger, P. Fischer, T. Brox, U-net: Convolutional networks for biomedical image segmentation, Lect. Notes Comput. Sci.(Including Subser. Lect. Notes Artif. Intell. Lect. Notes Bioinformatics). 9351 (2015) 234–241.
- [10] Z. Zhou, M.M.R. Siddiquee, N. Tajbakhsh, J. Liang UNet++: Redesigning Skip Connections to Exploit Multiscale Features in Image Segmentation IEEE Trans. Med. Imaging., 39(2020), pp. 1856-1867.L.C. Chen, Y. Zhu, G. Papandreou, F. Schroff, H. Adam, Encoder-decoder with atrous separable convolution for semantic image segmentation, Lect. Notes Comput. Sci. (Including Subser. Lect. Notes Artif. Intell. Lect. Notes Bioinformatics). 11211 LNCS (2018)833–851.
- [11] A. Baccouche, B. Garcia-Zapirain, C. Castillo Olea, A.S. Elmaghraby Connected-UNets: a deep learning architecture for breast mass segmentation, Npj Breast Cancer, 7(2021), pp. 1-12.
- [12] N.K. Tomar, A. Shergill, B. Rieders, U. Bagci, D. Jha, TransResU-Net: Transformer based ResU Net for Real-Time Colonoscopy PolypSegmentation, ArXiv. (2022) 1–4.
- [13] Garrucho, K. Kushibar, S. Jouide, O. Diaz, L. Igual, K. Lekadir Domain generalization in deep learning based mass detection in mammography: large-scale multicenter study Artif. Intell. Med., 132(2022), Article 102386.
- [14] Nabil Ibtehaz, M. Sohel Rahman. MultiResUNet: Rethinking the U-Net architecture for multimodal biomedical image segmentation. Networks <u>Volume</u> 121, Pages 74-87, January 2020.
- [15] A. Shrestha, A. Mahmood, Review of deep learning algorithms and architectures, IEEE Access 7 (2019) 53040–53065.
- [16] J. Arevalo, F.A. Gonza´ lez, R. Ramos-Polla´ n, J.L. Oliveira, M. A.G. Lopez, Representation learning for mammography mass lesion classification with convolutional neural networks, Comput. Methods Programs Biomed. 127 (15) (2016) 248–257.
- [17] D. Abdelhafiz, C. Yang, R. Ammar, S. Nabavi, Deep convolutional neural networks for mammography: Advances, challenges and applications, BMC Bioinf. 20 (11) (2019) 1–20.
- [18] L. Tsochatzidis, L. Costaridou, I. Pratikakis, Deep learning for breast cancer diagnosis from mammograms—a comparative study, J. Imaging 5 (3) (2019) 37.
- [19] N. Alam, A. Oliver, E.R. Denton, R. Zwiggelaar, Automatic segmentation of microcalcification clusters, Annual Conference on Medical Image Understanding and Analysis, 894, Springer, Cham, 2018, pp. 251–261

- [20] S. Duraisamy, S. Emperumal, Computer-aided mammogram diagnosis system using deep learning convolutional fully complex-valued relaxation neural network classifier, IET Comput. Vis., 11 (8) (2017) 656–662.
- [21] E. Deniz, A. S\_engu"r, Z. Kadirog" lu, Y. Guo, V. Bajaj, U". Budak, Transfer learning based histopathologic image classification for breast cancer detection, Health Inform. Sci. Syst. (1) (2018) 1–7.
- [22] S. Kwok, Multiclass classification of breast cancer in whole-slide images, International conference image analysis and recognition, 10882, Springer, Cham, 2018, pp. 931–940.
- [23] Li, Chen, Dan Xue, Hu. Zhijie, Hao Chen, Yao. Yudong, Yong Zhang, Mo Li, Qian Wang, Xu. Ning, A Survey for breast histopathology image analysis using classical and deep neural networks, in International Conference on Information Technologies in Biomedicine. Springer, Cham, vol. 1011, 2019, pp. 222–233.
- [24] D.A. Ragab, M. Sharkas, S. Marshall, J. Ren, Breast cancer detection using deep convolutional neural networks and support vector machines, PeerJ 7 (4) (2019) e6201.
- [25] C. Liang, M. Li, Z. Bian, W. Lv, D. Zeng, J. Ma, Establishment of a deep feature-based classification model for distinguishing benign and malignant breast tumors on full-filed digital mammography, J. Southern Med. Univ. 39 (1) (2019) 88–92.
- [26] S.C. Wong, A. Gatt, V. Stamatescu, and M.D. McDonnell, Understanding data augmentation for classification: when to warp, in 2016 International Conference on Digital Image Computing: IEEE Techniques and Applications (DICTA), Gold Coast, QLD, Australia, pp. 1–6, 2016.
- [27] Y. Chen, T. Zheming, Z. Yang, S. Holly, L. Norford, Transfer learning with deep neural networks for model predictive control of HVAC and natural ventilation in smart buildings, J. Cleaner Prod. 254 (119866) (2020) 1–10.
- [28] M. S. Akter, H. Shahriar, S. Sneha and A. Cuzzocrea, "Multi-class Skin Cancer Classification Architecture Based on Deep Convolutional Neural Network," 2022 IEEE International Conference on Big Data (Big Data), Osaka, Japan, 2022, pp. 5404-5413, doi: 10.1109/BigData55660.2022.10020302.
- [29] Maity, S., Saha, D., Singh, P.K. *et al.* JUIVCDv1: development of a still-image-based dataset for Indian vehicle classification. *Multimed Tools Appl* (2024).
- [30] K. Simonyan, A. Zisserman, Very deep convolutional networks for large-scale image recognition, 2014, arXiv preprint arXiv:1409.1556.
- [31] C.D. Lekamlage, F. Afzal, E. Westerberg, A. Cheddad, Mini-DDSM: Mammography-based automatic age estimation, 2020, arXiv preprint arXiv:2010.00494.

- [32] K. He, X. Zhang, S. Ren, J. Sun, Deep residual learning for image recognition, in: Proceedings of the IEEE Conference on Computer Vision and Pattern Recognition, 2016, pp. 770–778.
- [33] Ange Lou, Shuyue Guan, and Murray Loew "DC-UNet: rethinking the U-Net architecture with dual channel efficient CNN for medical image segmentation", Proc. SPIE 11596, Medical Imaging 2021: Image Processing, 115962T (15 February 2021)
- [34] Christian Szegedy, Vincent Vanhoucke, Sergey Ioffe, Jon Shlens, and Zbigniew Wojna. Rethinking the inception architecture for computer vision. In Proceedings of the IEEE conference on computer vision and pattern recognition, pages 2818-2826, 2016.
- [35] S. Targ, D. Almeida, K. Lyman, Resnet in Resnet: Generalizing residual architectures, In International Conference on Learning Representations, ICLR 2016, San Juan, Puerto Rico, 2-4 May, pp. 1–4, 2016.
- [36] X. Zhang, J. Zou, K. He, J. Sun, Accelerating very deep convolutional networks for classification and detection, IEEE Trans. Pattern Anal. Mach. Intell. 38 (10) (2015) 1943–1955.
- [37] H. Shin, H.R. Chang, G. Roth, L. Lu, X. Mingchen, I. Ziyue, Y. Nogues, D. Jianhua, Mollura, R.M. Summers, Deep convolutional neural networks for computer-aided detection: CNN architectures, dataset characteristics and transfer learning, IEEE Trans. Med. Imaging, 35 (5) (2016) 1285–1298.
- [38] S. Sasikala, M. Bharathi, M. Ezhilarasi, M. Ramasubba Reddy, S. Arunkumar, Fusion of MLO and CC view binary patterns to improve the performance of breast cancer diagnosis, Curr. Med. Imaging 14 (4) (2018) 651–658.
- [39] Chapala, H., &Sujatha, B. (2020, July). ResNet: Detection of Invasive Ductal Carcinomain Breast Histopathology Images Using Deep Learning. In2020 International Conference on Electronics and Sustainable Communication Systems (ICESC)(pp. 60-67).IEEE.
- [40] M. Sandler, A. Howard, M. Zhu, A. Zhmoginov, L.-C. Chen, Mobilenetv2: Inverted residuals and linear bottlenecks, in: Proceedings of the IEEE Conference on Computer Vision and Pattern Recognition, 2018, pp. 4510–4520.
- [41] K. Balaji. "Image Augmentation based on Variational Autoencoder for Breast Tumor Segmentation", Academic Radiology, 2023.
- [42] Heath, M.; Bowyer, K.; Kopans, D.; Kegelmeyer, P.; Moore, R.; Chang, K.; Munishkumaran, S. Current status of the digital database for screening mammography. In Digital Mammography; Springer: Cham, Switzerland, 1998; pp. 457–460.
- [43] Ozkaraca O, Bağrıacık Oİ, Guruler H, Khan F, Hussain J, Khan J, Ue Laila (2023) Multiple brain

- tumor classification with dense cnn architecture using brain mri images. Life 13(2):349.
- [44] Asad R, Rehman SU, Imran A, Li J, Almuhaimeed A, Alzahrani A (2023) Computer-aided early melanoma brain-tumor detection using deep-learning approach. Biomedicines 11(1):184.
- [45] Altheneyan A, Alhadlaq A (2023) Big data ml-based fake news detection using distributed learning. IEEE Access 11:29447–29463.
- [46] Alkaissy M, Arashpour M, Golafshani EM, Hosseini MR, Khan mohammadi S, Bai Y, Feng H (2023) Enhancing construction safety: machine learning-based classification of injury types. Safety Sci 162:106102.
- [47] Sahu A, Das P, Meher S High accuracy hybrid CNN classifiers for breast cancer detection using mammogram and ultrasound datasets *Signal Processing and Control*, (2023), 80.
- [48] K. Dong, C. Zhou, Y. Ruan and Y. Li, "MobileNetV2 Model for Image Classification," 2020 2nd International Conference on Information Technology and Computer Application (ITCA), Guangzhou, China, 2020, pp. 476-480, doi: 10.1109/ITCA52113.2020.00106.